ECCOMAS Congress 2016
VII European Congress on Computational Methods in Applied Sciences and Engineering
M. Papadrakakis, V. Papadopoulos, G. Stefanou, V. Plevris (eds.)
Crete Island, Greece, 5–10 June 2016

SHAPE OPIMIZATION OF GRAPHENE SHEETS FOR MAXIMUM FUNDAMENTAL FREQUENCY

Jin-Xing Shi [1] **and Masatoshi Shimoda** [2]

[1] Toyota Technological Institute
2-12-1 Hisakata, Tempaku-ku, Nagoya, Aichi 468-8511, Japan
shi@toyota-ti.ac.jp

[2] Toyota Technological Institute
2-12-1 Hisakata, Tempaku-ku, Nagoya, Aichi 468-8511, Japan
shimoda@toyota-ti.ac.jp

Keywords: Graphene sheets, Frame structure, Frequency, Shape optimization,.

Abstract. *Graphene sheets (GSs) have been proposed to be a base material for nanoelectro-mechanical systems (NEMS) because of their excellent mechanical and electrical behaviors. In this work, we carry out shape optimization of GSs to enhance their dynamic behaviors. According to the Tersoff-Brenner force field theory and a link between molecular mechanics and solid mechanics of C-C bond, we model GSs as continuum frame structures at first. Then, we optimize the shape of the atomistic finite element models based on a developed free-form optimization method for frame structures. In this optimization process, we use the fundamental frequency as objective function and maximize it under a volume constraint and considering repeated eigenvalue problem. We assume each equivalent continuum beam to vary in the off-axis direction to the centroidal axis, and derive the shape gradient functions for determining the optimal design velocity field. According to the derived optimal design velocity field, the shape optimization of GSs can be carried out without shape parametrization. The numerical results show that, the fundamental frequency of GSs can be significantly enhanced after shape optimization, which would be helpful for applying GSs in NEMS.*

1 INTRODUCTION

Vibrational properties of graphene sheets (GSs) deserve to be studied, because they may contribute to the application of GSs as NEMS resonators. Up to now, various continuum mechanical models have been proposed to study the vibration modes of GSs, such as frame structure model, shell/plate model, and beam model [1-4]. Shape optimization is a procedure to improve or enhance the performance of the structure by changing design parameters. Recently, the shape of GSs can be controlled by an external electric field [5] or chemically modifying the adherence of GSs on metal [6]. Hence, shape optimization of GSs can make an effective role to improve their mechanical behaviors.

In our previous work, we adopted the molecular mechanics (MM) method to construct the continuum frame work and carried out the shape optimum design of GSs in terms of the compliance minimization problem based on a free-form optimization method for frame structures [7]. In the present work, we extend this optimization method to the fundamental frequency maximization problem of GSs, and make shape optimum design of GSs.

We arrange this study as following. In section 2, we introduce the MM method for constructing the frame structures of GSs. In section 3, we develop a free-form shape optimization method for frame structures and introduce the shape optimization process for shape design of GSs. In section 4, using the developed shape optimization process, we carry out two examples to obtain the optimal shapes of GSs. At last, we remark conclusions in section 5.

2 SHAPE OPTIMIZATION OF GRAPHENE SHEETS

2.1 Governing equation

We introduce the MM method for modeling frame structure of GSs at first. In MM method, the forces between two individual atoms are depicted as continuum beam elements. We assume an equivalent C-C beam with a circular cross-section of diameter d and initial length 1.42 Å. According to the Tersoff-Brenner force field theory [8] and a link between molecular and solid mechanics of C-C bond, we derive the Young's modulus E_b, shear modulus G_b and diameter d as [9]:

$$E_b = \frac{k_l^2 l}{4\pi k_\theta},\ G_b = \frac{k_l^2 k_\tau l}{8\pi k_\theta^2},\ d = 4\sqrt{\frac{k_\theta}{k_l}} \tag{1}$$

where k_l = 93800 kcal/mol/nm^2, k_θ = 126 kcal/mol/rad^2, and k_τ = 40 kcal/mol/rad^2 are obtained by fitting to the structural and vibrational frequency data on small molecular fragments [10].

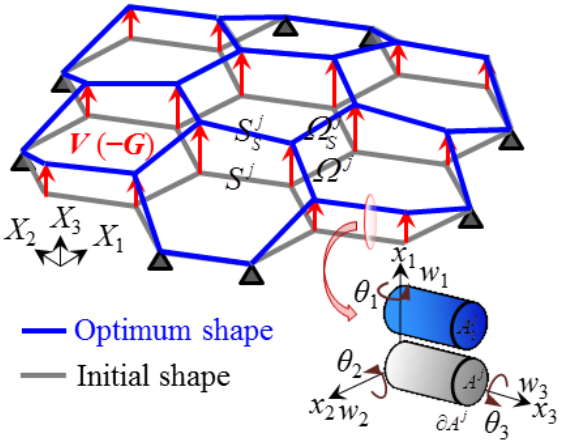

Figure 1: Shape variation of graphene sheets.

As shown in Fig. 2, a frame structure of GS with a bounded domain $\Omega \subset \mathbb{R}^3$ consists of Timoshenko beams Ω^j, $j=1,2,...,N$, where $\mathbb{R}$ is a set of positive real numbers and N is the number of beams. The notations (x_1, x_2, x_3) and (X_1, X_2, X_3) indicate the local coordinate system in terms of a Timoshenko beam and the global coordinate system, respectively.

$$\Omega^j = \left\{ \left(x_1^j, x_2^j, x_3^j \right) \in \mathbb{R}^3 \middle| \left(x_1^j, x_2^j \right) \in A^j \subset \mathbb{R}^2, x_3^j \in S^j \subset \mathbb{R} \right\},\ \Gamma^j = \partial A^j \times S^j,\ \Omega^j = A^j \times S^j \quad (2)$$

where S^j, Γ^j and Ω^j express the centroidal axis, circumference surface and whole domain of member *j*, respectively. A^j and ∂A^j are the cross section and its circumference of member *j*, respectively. The subscript *j* shall be omitted to avoid the complexity of expression in the sequel. $\boldsymbol{w} = \{w_i\}_{i=1,2,3}$ and $\boldsymbol{\theta} = \{\theta_i\}_{i=1,2,3}$ are the displacement vector and rotation vector in the x_1, x_2, x_3 directions of the local coordinate system, respectively. Then, the weak form governing equation of the eigenfrequency in terms of $(\boldsymbol{w}^{(r)}, \boldsymbol{\theta}^{(r)})$ can be expressed as

$$a\left(\left(\boldsymbol{w}^{(r)}, \boldsymbol{\theta}^{(r)} \right), \left(\bar{\boldsymbol{w}}, \bar{\boldsymbol{\theta}} \right) \right) = \lambda^{(r)} b\left(\left(\boldsymbol{w}^{(r)}, \boldsymbol{\theta}^{(r)} \right), \left(\bar{\boldsymbol{w}}, \bar{\boldsymbol{\theta}} \right) \right),\ \forall \left(\bar{\boldsymbol{w}}, \bar{\boldsymbol{\theta}} \right) \in U, \left(\boldsymbol{w}^{(r)}, \boldsymbol{\theta}^{(r)} \right) \in U \quad (3)$$

where $(\cdot)^{(r)}$ denotes the eigenvector of *r* th natural frequency mode and $\lambda^{(r)}$ denotes its eigenvalue (the square of the *r* th natural frequency). The notation $(\bar{\cdot})$ expresses a variation, and *U* is the admissible function space, in which the given constraint conditions of $(\boldsymbol{w}, \boldsymbol{\theta})$ are satisfied. In the frame structure of GSs as shown in Fig. 2, due to the domain variation $\boldsymbol{V}$ (design velocity field) in the out-of-plane direction, the initial domain Ω^j and a centroidal axis S^j of member *j* become Ω_s^j and S_s^j, respectively. The subscript *s* expresses the iteration history of the domain variation. Moreover, the bilinear form $a(\cdot,\cdot)$ and $b(\cdot,\cdot)$ are the rigidity item and inertia item, respectively.

2.2 Fundamental frequency maximization problem

The free-form optimization method for frame structures is adopted to maximize the natural frequency of GSs, and is formulated as

$$\text{Given} \quad \Omega \quad (4)$$

$$\text{Find} \quad \boldsymbol{V} \quad (5)$$

$$\text{that minimizes} \quad -\lambda^{(1)} \quad (6)$$

$$\text{subject to} \quad \text{Eq. (3) and} \quad M\left(= \sum_{j=1}^{N} \int_{S^j} A dS \right) \le \hat{M} \quad (7)$$

where *M* and $\hat{M}$ are the volume of a GS and its constraint value, respectively.

Letting $(\bar{\boldsymbol{w}}, \bar{\boldsymbol{\theta}})$ and Λ denote the Lagrange multipliers for the governing equation and volume constraint, respectively, the Lagrange functional *L* associated with the fundamental frequency maximization problem can be expressed as

$$\begin{aligned} L\left(\Omega, \left(\boldsymbol{w}^{(1)}, \boldsymbol{\theta}^{(1)} \right), \left(\bar{\boldsymbol{w}}, \bar{\boldsymbol{\theta}} \right), \Lambda \right) = & -\lambda^{(1)} + \lambda^{(1)} b\left(\left(\boldsymbol{w}^{(1)}, \boldsymbol{\theta}^{(1)} \right), \left(\bar{\boldsymbol{w}}, \bar{\boldsymbol{\theta}} \right) \right) \\ & - a\left(\left(\boldsymbol{w}^{(1)}, \boldsymbol{\theta}^{(1)} \right), \left(\bar{\boldsymbol{w}}, \bar{\boldsymbol{\theta}} \right) \right) + \Lambda\left(M - \hat{M} \right) \end{aligned} \quad (8)$$

The material derivative $\dot{L}$ of the Lagrange functional is derived as

$$\begin{aligned}\dot{L} = {} & \dot{\lambda}^{(1)}\left\{b\left(\left(\boldsymbol{w}^{(1)},\boldsymbol{\theta}^{(1)}\right),\left(\bar{\boldsymbol{w}},\bar{\boldsymbol{\theta}}\right)\right)-1\right\}+\lambda^{(1)}b\left(\left(\boldsymbol{w}^{(1)\prime},\boldsymbol{\theta}^{(1)\prime}\right),\left(\bar{\boldsymbol{w}},\bar{\boldsymbol{\theta}}\right)\right)\\ & +\lambda^{(1)}b\left(\left(\boldsymbol{w}^{(1)},\boldsymbol{\theta}^{(1)}\right),\left(\bar{\boldsymbol{w}}',\bar{\boldsymbol{\theta}}'\right)\right)-a((\boldsymbol{w}^{(1)\prime},\boldsymbol{\theta}^{(1)\prime}),(\bar{\boldsymbol{w}},\bar{\boldsymbol{\theta}}))-a((\boldsymbol{w}^{(1)},\boldsymbol{\theta}^{(1)}),(\bar{\boldsymbol{w}}',\bar{\boldsymbol{\theta}}'))\\ & +\dot{\Lambda}\left(M-\hat{M}\right)+\langle G\boldsymbol{n},\boldsymbol{V}\rangle,\ \boldsymbol{V}\in C_{\Theta}\end{aligned} \tag{9}$$

where $G\boldsymbol{n}$ ($\equiv \boldsymbol{G}$) expresses the shape gradient function (i.e., sensitivity function), which is a coefficient function in terms of $\boldsymbol{V}$. $\boldsymbol{n}$ is the outward unit normal vector on the circumference surface Γ or a unit normal vector on the centroidal axis S. The notations $(\cdot)'$ and $\dot{(\cdot)}$ are the shape derivative and the material derivative with respect to the domain variation, respectively.

The optimum conditions of the Lagrange functional L with respect to $(\boldsymbol{w}^{(1)},\boldsymbol{\theta}^{(1)})$, $(\bar{\boldsymbol{w}},\bar{\boldsymbol{\theta}})$, and Λ are shown as

$$a\left(\left(\boldsymbol{w}^{(1)},\boldsymbol{\theta}^{(1)}\right),\left(\bar{\boldsymbol{w}}',\bar{\boldsymbol{\theta}}'\right)\right)=\lambda^{(1)}b\left(\left(\boldsymbol{w}^{(1)},\boldsymbol{\theta}^{(1)}\right),\left(\bar{\boldsymbol{w}}',\bar{\boldsymbol{\theta}}'\right)\right),\ \ \forall\left(\bar{\boldsymbol{w}}',\bar{\boldsymbol{\theta}}'\right)\in U \tag{10}$$

$$a\left(\left(\boldsymbol{w}^{(1)\prime},\boldsymbol{\theta}^{(1)\prime}\right),\left(\bar{\boldsymbol{w}},\bar{\boldsymbol{\theta}}\right)\right)=\lambda^{(1)}b\left(\left(\boldsymbol{w}^{(1)\prime},\boldsymbol{\theta}^{(1)\prime}\right),\left(\bar{\boldsymbol{w}},\bar{\boldsymbol{\theta}}\right)\right),\ \ \forall\left(\boldsymbol{w}^{(1)\prime},\boldsymbol{\theta}^{(1)\prime}\right)\in U \tag{11}$$

$$b\left(\left(\boldsymbol{w}^{(1)},\boldsymbol{\theta}^{(1)}\right),\left(\bar{\boldsymbol{w}},\bar{\boldsymbol{\theta}}\right)\right)=1 \tag{12}$$

$$\dot{\Lambda}\left(M-\hat{M}\right)=0\ \ M-\hat{M}\le 0\ \ \Lambda\ge 0 \tag{13}$$

When the optimality conditions are satisfied, considering the self-adjoint relationship $(\boldsymbol{w}^{(1)},\boldsymbol{\theta}^{(1)})=(\bar{\boldsymbol{w}},\bar{\boldsymbol{\theta}})$, we get

$$\dot{L}=\langle G\boldsymbol{n},\boldsymbol{V}\rangle=\sum_{j=1}^{N}\int_{S^j}\left\{G_1\boldsymbol{V}\cdot\boldsymbol{n}_1+G_2\boldsymbol{V}\cdot\boldsymbol{n}_2+G_0\boldsymbol{V}\cdot\boldsymbol{n}\right\}dS \tag{14}$$

where the shape gradient functions G_1, G_2, and G_0 are applied in the free-form optimization method for frame structures of GSs to determine the optimal design velocity field $\boldsymbol{V}$.

2.3 Free-form optimization method and repeated eigenvalue problem

The free-form optimization method for frame structures was proposed by Shimoda [11]. In this method, the negative shape gradient function $-\boldsymbol{G}(=-G\boldsymbol{n})$ is applied as a distributed force in the off-axis direction to the centroidal axis of a fictitious-elastic frame structure under a Robin condition (spring constant α). This makes it possible both to reduce the objective functional and to maintain smoothness, i.e., mesh regularity, simultaneously. The optimal shape variation, or the optimal design velocity field $\boldsymbol{V}$ is determined as the displacement field in this pseudo-elastic frame analysis, and the obtained $\boldsymbol{V}$ is used to update the shape. This analysis is called velocity analysis. The governing equation of the velocity analysis is shown as

$$a\left((\boldsymbol{V},\boldsymbol{\theta}),\left(\bar{\boldsymbol{w}},\bar{\boldsymbol{\theta}}\right)\right)+\alpha\left\langle(\boldsymbol{V}\cdot\boldsymbol{n})\boldsymbol{n},\left(\bar{\boldsymbol{w}},\bar{\boldsymbol{\theta}}\right)\right\rangle=-\left\langle G\boldsymbol{n},\left(\bar{\boldsymbol{w}},\bar{\boldsymbol{\theta}}\right)\right\rangle,\ \forall\left(\bar{\boldsymbol{w}},\bar{\boldsymbol{\theta}}\right)\in C_{\Theta},\ (\boldsymbol{V},\boldsymbol{\theta})\in C_{\Theta} \tag{15}$$

$$C_{\Theta}=\left\{(V_1,V_2,V_3,\theta_1,\theta_2,\theta_3)\in\left(H^1(S)\right)^6\,\middle|\,\text{satisfy Dirichlet condition for shape variation}\right\} \tag{16}$$

In design problems where convexity is assured, this relationship definitely reduces the Lagrange functional in the process of updating the shape of GSs using the design velocity field

$\boldsymbol{V}$ determined from Eq. (15). The shape optimization process for frame structure of GSs is constructed by repeating the vibration analysis, calculation of the shape gradient functions, velocity analysis, and shape updating. The vibration analysis and velocity analysis are carried out using a standard commercial FEM code.

We also consider the repeated eigenvalue problem in this study. When the repeated eigenvalue problem happens, we change the objective and constraint functions to the summation forms as shown in the first term of the right side of Eq. (17). The notation r (≥ 2) denotes the multiplicity of the repeated eigenvalues. The occurrence of repeated eigenvalue is judged with a tolerance δ, and we set $\delta = \{_{-0}^{+0.02\lambda^{(1)}}$ in the present work.

$$\begin{aligned} &L((\boldsymbol{w}^{(1)},\boldsymbol{\theta}^{(1)}),\cdots,(\boldsymbol{w}^{(r)},\boldsymbol{\theta}^{(r)}),(\bar{\boldsymbol{w}}^{(1)},\bar{\boldsymbol{\theta}}^{(1)})\cdots,(\bar{\boldsymbol{w}}^{(r)},\bar{\boldsymbol{\theta}}^{(r)}),\Lambda) \\ &=\sum_{k=1}^{r}\left\{-\lambda^{(k)}+\lambda^{(k)}b((\boldsymbol{w}^{(k)},\boldsymbol{\theta}^{(k)}),(\bar{\boldsymbol{w}}^{(k)},\bar{\boldsymbol{\theta}}^{(k)}))-a((\boldsymbol{w}^{(k)},\boldsymbol{\theta}^{(k)}),(\bar{\boldsymbol{w}}^{(k)},\bar{\boldsymbol{\theta}}^{(k)}))\right\}+\Lambda(M-\hat{M}) \end{aligned} \tag{17}$$

In an analogous way, the shape gradient functions should be replaced as

$$G_1=\sum_{k=1}^{r}G_1^{(k)},\quad G_2=\sum_{k=1}^{r}G_2^{(k)} \tag{18}$$

3 OPTIMIZATION RESULTS OF GRAPHENE SHEETS

In order to evaluate the shape optimization process of GSs for enhancing their fundamental frequency, we carry out two numerical examples to optimize the shape of a graphene nanoribbon (GNR) and an irregular GS. The volume constraint is set to be $M \leq \hat{M} = 1.005 M_{\text{initial}}$, where M_{initial} is the initial volume of GSs. It should be noted that the constraint conditions are set as 1 (x_1 direction), 2 (x_2 direction), 3 (x_3 direction), 4 (θ_1 direction), 5 (θ_2 direction) and 6 (θ_3 direction) in the present work.

3.1 Shape optimization of a graphene nanoribbon

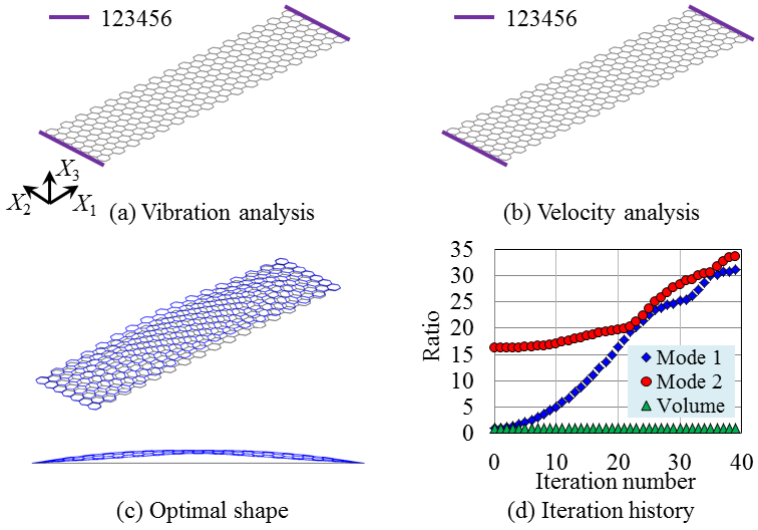

Figure 2: Shape optimization of a graphene nanoribbon.

In the first example, we design the shape a GNR shown in Fig. 2 with 510 carbon atoms and 724 equivalent C-C beams. As shown in Fig. 2 (a) and (b), two ends of the GNR are con-

strained in 123456 in both of the vibration analysis and the velocity analysis. Furthermore, to assure that all carbon atoms are varied in the X_3 direction, all of the remained nodes in velocity analysis are constrained in 12. We carry out shape optimization of the GNR by using the developed shape optimization process, and show the optimal shape and the iteration history in Fig. 2 (c) and (d), respectively. With respect to the optimal shape shown in Fig. 2 (c), the middle of the GNR becomes convex to enhance its fundamental frequency, and the optimal shape of the GNR is smooth, which is a feature of the free-form shape optimization method. In the iteration history shown in Fig. 2 (d), the fundamental frequency (mode 1) is enhanced smoothly while satisfying the volume constraint $M \le \hat{M} = 1.005 M_{\text{initial}}$, and the repeated eigenvalue problem occurs from the 22th iteration. This shape optimization process converges at the 39th iteration, and the fundamental natural frequency (mode 1) is enhanced to 31.15 times to the initial shape.

3.2 Shape optimization of an irregular graphene sheet

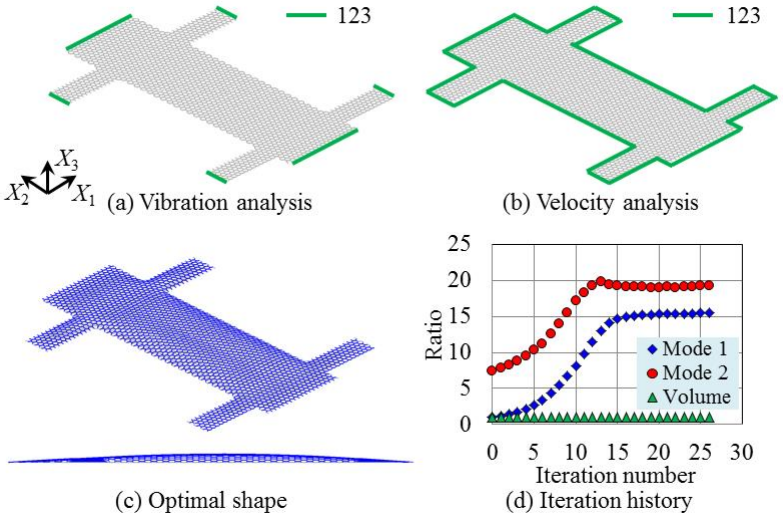

Figure 3: Shape optimization of an irregular graphene sheet.

We design an irregular GS shown in Fig. 3 containing 3194 carbon atoms and 4636 equivalent C-C beams in the example 2. We show the constraint condition of the vibration analysis and the velocity analysis in Fig. 3 (a) and (b), respectively. Using the proposed shape optimization process, the optimal shape of the GS is shown in Fig.3 (c). From the iteration history shown in Fig. 3 (d), the repeated eigenvalue problem does not occurs in this example, and the fundamental frequency of the GS is enhanced to 15.45 times to the initial shape in the 26th iteration, while the volume constraint is satisfied.

4 CONCLUSIONS

In this work, we developed a shape optimization system of GSs for the fundamental frequency maximization problem. At first, based on the MM method, GSs were modeled as frame structures composed of Timoshenko beams. Next, the fundamental frequency maximization problem of the frame structure of GSs was formulated. We adopted the free-form shape optimization method for frame structures to achieve the optimal shapes of GSs. This method has advantages that the optimal shapes of GSs could be determined smoothly and without requiring shape design parameterization. The objective of the shape optimization process was to maximize the fundamental frequency of GSs under the volume constrain. We also considered

the repeated eigenvalue problem in the present work. Two design examples were carried out to confirm the effectiveness of the developed shape optimization process, and the results showed that the obtained optimal shapes in both of the two design examples were smooth and the fundamental frequency of each example was enhanced significantly.

ACKNOWLEDGEMENT

This work was supported by JSPS KAKENHI Grant Number 15K21485 and grants in-aid from the Research Center of Smart and Tough Machines at Toyota Technological Institute.

REFERENCES

[1] A. Shakouri, T.Y. Ng, R.M. Lin, A new REBO potential based atomistic structural model for graphene sheets. *Nanotechnology*, **22**, 295711, 2011.

[2] J.B. Wang, X.Q. He, S. Kitipornchai, H.W. Zhang, Geometrical nonlinear free vibration of multi-layered graphene sheets. *Journal of Physics D: Applied Physics*, **44**, 135401 2011.

[3] J.X. Shi, Q.Q. Ni, X.W. Lei, T. Natsuki, Nonlocal vibration analysis of nanomechanical systems resonators using circular double-layer graphene sheets. *Applied Physics A*, **115**, 213-219, 2014.

[4] J.X. Shi, Q.Q. Ni, X.W. Lei, T. Natsuki, Nonlocal vibration of embedded double-layer graphene nanoribbons in in-phase and anti-phase modes. *Physica E: Low-dimensional Systems and Nanostructures*, **44**, 1136-1141, 2012.

[5] T. Georgiou, L. Britnell, P. Blake, R.V. Gorbachev, A. Gholinia, A.K. Geim, C. Casiraghi, K.S. Novoselov, Graphene bubbles with controllable curvature. *Applied Physics Letters*, **99**, 093103, 2011.

[6] J. Lu, A.H. Castro Neto, K.P. Loh, Transforming moiré blisters into geometric graphene nano-bubbles. *Nature Communications*, **3**, 823, 2012.

[7] J.X. Shi, M. Shimoda, Shape optimum design of graphene sheets. *Proceedings of 11th World Congress on Structural and Multidisciplinary Optimisation (WCSMO-11)*, Sydney, Australia, June 7-12, 2015.

[8] A.K. Rappe, C.J. Casewit, K.S. Colwell, W.A. Goddard III, W.M. Skiff, UFF, a full periodic table force field for molecular mechanics and molecular dynamics simulations. *Journal of the American Chemical Society*, **114**, 10024-10035, 1992.

[9] J.X. Shi, T. Natsuki, X.W. Lei, Q.Q. Ni, Equivalent Young's modulus and thickness of graphene sheets for the continuum mechanical models. *Applied Physics Letters*, **104**, 223101, 2014.

[10] W.D. Cornell, P. Cieplak, C.I. Bayly, I.R. Gould, K.M. Merz, D.M. Ferguson, D.C. Spellmeyer, T. Fox, J.W. Caldwell, P.A. Kollman, A second generation force field for the simulation of proteins, nucleic acids, and organic molecules. *Journal of the American Chemical Society*, **117**, 5179-5197, 1995.

[11] M. Shimoda, Y. Liu, T. Morimoto, Non-parametric free-form optimization method for frame structures. *Structural and Multidisciplinary Optimization*, **50**, 129-146, 2014.